X-ray absorption spectroscopy of the cubic and hexagonal polytypes of zinc sulfide

B. Gilbert,[1,*] B. H. Frazer,[1,2] H. Zhang,[3] F. Huang,[3] J. F. Banfield,[3] D. Haskel,[4] J. C. Lang,[4] G. Srajer,[4] and G. De Stasio[1]
[1]*University of Wisconsin, Department of Physics, and Synchrotron Radiation Center, 3731 Schneider Drive, Stoughton, Wisconsin 53589*
[2]*Institut de Physique Appliquée, Ecole Polytechnique Fédéral de Lausanne, CH-1015 Lausanne, Switzerland*
[3]*Department of Geology and Geophysics, University of Wisconsin-Madison, Wisconsin*
[4]*Advanced Photon Source, Argonne National Laboratory, Argonne, Illinois 60439*
(Received 18 June 2002; published 26 December 2002)

We investigate the sensitivity of x-ray absorption spectroscopy to *cubic-hexagonal* polytypism in which nearest-neighbor positions are virtually unchanged. Experimental spectra and multiple-scattering calculations are reported at the major absorption edges in the zinc-blende and wurtzite modifications of ZnS. We demonstrate that *d*-like unoccupied bands are preferentially affected, as only *L*-edge absorption is sensitive to this structural transition. The results allow near-edge x-ray absorption spectroscopy to be evaluated as a detection method for crystal structure modifications in nano-scale systems.

DOI: 10.1103/PhysRevB.66.245205 PACS number(s): 71.20.Nr, 78.70.Dm

I. INTRODUCTION

X-ray absorption spectroscopy (XAS) is widely used to investigate bonding, coordination number, and valence, but no systematic work has appeared in the literature that investigates the sensitivity of x-ray absorption near-edge structure (XANES) to subtle structural modifications in which the nearest-neighbor environment is unchanged. Many tetrahedrally bonded crystalline materials are found to be stable in two or more stacking arrangements, that is, polytypes, in which structural units are combined in alternative ways. Several important classes of semiconducting materials exhibit *cubic-hexagonal* polytypism, which can be very close in total energy,[1] yet possess different structural and electrical properties such as density, electronic band gap, and luminescence efficiency.[2] ZnS is of interest as a phosphor and electroluminescent material, and is a system in which electrical and structural properties are being investigated as a function of particle size.[3] Sphalerite, the *cubic* (zinc blende) form of ZnS is stable at room temperature, while wurtzite, the less dense *hexagonal* form, is stable above 1020 °C at atmospheric pressure and metastable as a macroscopic phase under ambient conditions. The relative stability of these phases is modified in both synthetic and natural ZnS nanoparticles.[4,5] As a short-range structural probe, XAS is likely to be valuable in detecting crystal structure modifications in nanoscale systems, and additionally describes unoccupied electronic states, important in excited-state processes, such as optical absorption, luminescence, and photocatalysis. Some XANES studies on sulfides have included one ZnS polytype, or both but without the resolution to distinguish the fine structure at any absorption edge.[6–10]

A. Crystal structure of cubic and hexagonal ZnS

Two illustrations of the crystal structures of sphalerite (*cubic* or zinc blende phase) and wurtzite (*hexagonal*) are given in Fig. 1. When the comparison of *cubic*, along the [111] axis, to *hexagonal*, along the [1000] axis, is made, as in Fig. 1, a simple description of the difference between the structures is in the stacking order of {ZnS} layers-respectively *ABCA* and *ABA*.[11]

B. XAS as a probe of crystal structure

In x-ray absorption spectroscopy, a bound electron absorbs an x-ray photon and is consequently excited to an unoccupied state of the photoexcited system. Transitions to either bound or free final states which satisfy energy conservation, $h\nu = E_f - E_i$, are permitted, subject to dipole selection rules. Transitions to bound states can be considered probes of unoccupied atomic or molecular orbitals; transitions to propagating electron final states can be considered probes of the local geometry, which gives sensitivity to crystal structure. A propagating spherical photoelectron wave scatters coherently from surrounding atoms, and interference effects in the vicinity of the absorbing atom lead to modulations in the absorption cross section that vary with the photon energy. This is the basis for real-space photoelectron

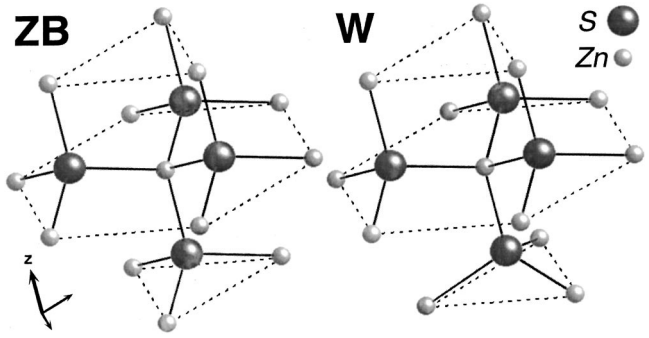

FIG. 1. Structures of zinc blende (ZB) and wurtzite (*W*) modifications of ZnS. From the central zinc atom, the second nearest neighbor shell is displayed. The crystals are aligned so the [111] axis (ZB) and the *c* axis (*W*) are parallel to the *z* axis indicated. Along these directions, the polytypes can be simply described as alternate stacking sequences of {Zn,S} layers following an ABA pattern in wurtzite and an *ABCA* pattern in zinc blende. The top and bottom S_3 triangles indicated in the figure are eclipsed (staggered) in wurtzite (zinc blende).

scattering approaches to x-ray absorption structure such as the FEFF code,[12] recently enhanced to perform full multiple-scattering calculations.

X-ray absorption spectroscopies are traditionally divided into near-edge and above-threshold regimes. Here we consider the near-edge regime, but briefly discuss the sensitivity of extended x-ray absorption fine-structure (EXAFS) spectroscopy to *cubic-hexagonal* polytypism. EXAFS experiments obtain information on the radial distribution of neighboring atoms, and nearest neighbor distances can be measured to below 0.01-Å accuracy. Structurally, however, zinc blende and wurtzite differ by more than this margin only at the third shell. This does allow the polytypes to be directly distinguished with data of sufficient quality; alternatively, *cubic* and *hexagonal* modifications are distinguished by observing the asymmetry of the interatomic cation-anion pair distribution.[15] Close to threshold, XANES is dominated by multiple-scattering (MS) events and probes farther from the absorbing atom. The study of the sensitivity of XAS to polytypism allows a consideration of the volume probed in the x-ray absorption process, relevant, for instance, to XAS in nanoscale materials.

II. EXPERIMENTAL METHODS

Fragments of natural zinc blende and synthetic wurtzite were mechanically powered to a grain size of greater than one micron, and x-ray diffraction of the resulting preparations showed pure phases of bulk material. A portion of the powders were pressed into indium metal and analyzed with x-ray absorption spectroscopy at the sulfur *L*-edge (0.2-eV photon energy resolution), zinc *L*-edge (0.3-eV resolution), and sulfur *K*-edge (0.5-eV resolution) in the total electron yield mode at the University of Wisconsin Synchrotron Radiation Center. Zinc *K*-edge data ($<$0.5-eV resolution) were acquired in fluorescence yield mode at the Advanced Photon Source, Argonne, IL.

III. THEORETICAL CALCULATIONS

X-ray absorption calculations were performed with FEFF 8.0,[12] with input structures generated by ATOMS,[13] and the following parameters gave best agreement with the experimental data. Zn and S muffin-tin potentials were calculated self consistently within 5-Å radius clusters around the Zn and S atoms, with the interstitial potential reduced by the factor 1.54. The muffin tins were overlapped, which is anticipated to give a better description of the covalent bonding in ZnS, and which gave best agreement with the data. We checked our conclusion that the XAS fine structure modifications were indeed due to long-range crystal structure differences by recalculating the wurtzite spectra using the muffin tin potentials derived for sphalerite. The wurtzite XANES were unaffected.

The calculated spectra were obtained with full multiple scattering up to $l=3$ or 2 angular momentum projected partial waves. For computational reasons, calculations for clusters $>$400 atoms were restricted in the angular momentum basis of the self consistent potentials to $l=2$. Good agreement farther in energy from the absorption threshold requires $l>2$, while close to threshold a large cluster size is more significant. Fully relaxed core hole potentials were used for S and Zn *K* edges. The core hole was fully shielded for S and Zn *L* edges. The Hedin-Lundqvist exchange potential gave the best results at all edges, although we note that the Dirac-Hara exchange potential has been previously reported to be optimal for Zn *K*-edge absorption in ZnS.[10]

TABLE I. Summary of FEFF full multiple-scattering (FMS) cluster sizes for XANES and DOS calculations of zinc blende (ZB) and wurtzite (*W*), and the maximum angular momentum in the partial wave expansion (*l*), corresponding to Figs. 2 and 3. The FMS XANES calculations converged at the cluster sizes shown. All muffin-tin potential calculations were performed with a cluster radius of 5 Å.

Calculation	FMS cluster radius (Å)		*l*
	ZB	*W*	
S $L_{2,3}$ XANES	13.89	14.11	2
Zn $L_{2,3}$ XANES	11.1	11.7	3
S *K* XANES	10.2	10.34	3
Zn *K* XANES	9.7	9.7	3
p DOS	11.5	12.27	2

FEFF calculations of near edge absorption structure are very sensitive to cluster size, and we tested for MS convergence at each absorption edge with cluster sizes up to a 14.11-Å radius (approximately 600 atoms). All calculations converged within this radius. They were performed increasing the number of sulfur atom outer shells, and convergence was defined as identical results for two successive cluster sizes. The cluster sizes used for the calculations are summarized in Table I.

The *l*-projected ground-state ZnS density of states (calculated once convergence and best agreement with absorption spectra had been obtained) were calculated with no core hole. The radii of the clusters used in the calculations are 11.5 Å (zinc blende, 329 atoms) and 12.27 Å (wurtzite, 406 atoms). It is important to consider the applicability of FEFF to *L*-edge absorption, because of the neglect by local density methods of multiplet interactions that can introduce significant structure in transition element *L*-edge absorption spectra. S 3*d* and Zn 4*d* bands are unoccupied, and hence *d*-*d* interactions are absent. This leaves core hole $2p$-$3d$ interactions, observable in, e.g., Ca *L*-edge absorption,[16] but which appear not to be significant in ZnS, seen from the close agreement between calculation and experiment. We concluded that there is little interaction between the excited *d* states and the core *p* hole, as better agreement with experimental data was obtained by completely screening the core hole in the calculations. Spectra from the spin-orbit split initial *p* states of S (1.1-eV separation) and Zn (23.1 eV) were therefore calculated independently, and combined to reproduce the full $L_{2,3}$ edges. It has been shown that a prethreshold feature in CdS sulfur XANES corresponds to excitation to a core exciton,[17] a phenomenon not included in the MS calculations. This has been empirically included in the simulated sulfur spectrum by a Gaussian peak fitted to the first 3 eV of the experimental

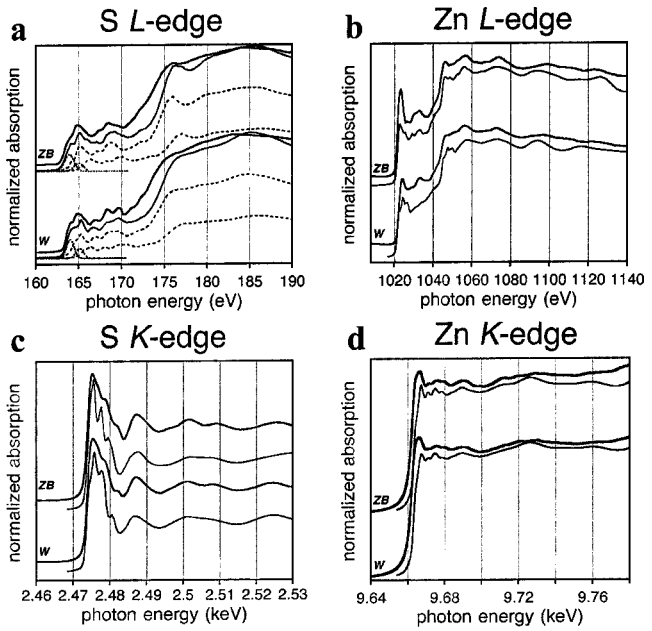

FIG. 2. Experimental and calculated XANES of ZnS zinc blende (ZB) and wurtzite (*W*) polytypes. For each polytype, the upper thick curve is the experiment and the lower thin curve is the calculation. Clockwise from top: (a) S *L*-edge. The sulfur $2p$ spin-orbit splitting is 1.1 eV and the full $L_{2,3}$ spectrum is displayed, including L_2, L_3, and exciton prepeak components (dashed lines). (b) Zn *L*-edge. The zinc $2p$ spin-orbit splitting is 23.1 eV and the calculated full $L_{2,3}$ spectrum is displayed. (c) S *K*-edge. (d) Zn *K*-edge.

spectra. We show that by including both *L* components and excitons we obtained an excellent agreement with the low-energy spectra of both polytypes.

IV. RESULTS AND DISCUSSION

A. XANES of ZnS polytypes

The experimental data are given in Fig. 2, compared to full multiple scattering calculations of x-ray absorption. The experimental XANES of the ZnS polytypes give clearly resolved experimental x-ray absorption line shapes at each *L*-edge, while the lineshapes are indistinguishable at the sulfur and zinc *K* edges, and this behavior is very closely reproduced by calculation. At the S *L*-edge [Fig. 2(a)] our spectrum of *cubic* ZnS agrees well with previous data,[7] and the *hexagonal* ZnS is strikingly similar to *hexagonal* CdS absorption.[19] In another previous study, S *L*-edge XANES of zinc-blende and wurtzite ZnS are shown to be indistinguishable,[6] in disagreement with our results, probably due to better energy resolution in our data.

The converged multiple scattering calculations generally reproduce all features in the XANES line shapes, with some discrepancies in energy position and relative intensities. The energy separation of the absorption features is related to the real part of the photoelectron self-energy,[14] and Fig. 2 shows that the Hedin-Linqvist exchange-correlation potential gives excellent agreement with the data for core hole energies ranging from 160 eV to 10 keV. Immediately post-edge on the S and Zn *K*-edge spectra [Figs. 2(c) and 2(d)], the fine structure appears too close to the main peak by 1 eV or less. Slightly better agreement is obtained in this region with the use of the Dirac-Hara potential,[10] but the neglect of inelastic losses gives overall worse agreement to the data. There are discrepancies between data and calculation for Zn *L*-edge XANES of the wurtzite polytype, as a major post-threshold feature appears to be completely absent. In fact, features are predicted in the correct energy position, but are too weak. The lower Zn and S site symmetries in wurtzite compared to zinc blende (ZB) reduce the photoelectron scattering path degeneracies, but despite the previous example, the calculated wurtzite XANES are equal in quality to the sphalerite results overall.

To understand the orbital dependence of polytype sensitivity, in Fig. 3 we present the calculated density of states (DOS) of the two polytypes, explicitly showing as an inset the *s*-, *p*-, and *d*-projected unoccupied DOS's at the sulfur atom. Ultraviolet and x-ray photoemission studies, and soft-x-ray fluorescence have shown that the valence band (VB) of II/VI compounds is separated into a mostly anion $3p$-derived upper VB, and a mostly anion $3s$-derived lower VB.[18,19] This is reproduced by the present calculations, and a detailed composition of the conduction band is shown in Fig. 3. Going from ZB to *W*, the *d*-like conduction band states in the region 4–11 eV above the conduction band minimum are split. The spreading and appearance of peaks is observed experimentally in the S *L*-edge XANES [Fig. 2(a)] and indicates removal of degeneracy, consistent with lower site symmetry in the wurtzite crystal. Energy shifts occur on the order of 0.5 eV, almost an order of magnitude greater than analogous behavior observed in the valence band.[27] The *p*-like VB maximum at $k=0$ is degenerate in zinc blende (neglecting spin-orbit splitting), but splits in wurtzite due to the perturbation of non-nearest neighbor atoms that lower the site symmetry from T_d to C_{3v}. The magnitude of this VB splitting is less than 0.1 eV.

The sphalerite and wurtzite density of states of Fig. 3 can be compared with experimental evaluations and other calculations of the semiconducting band gap and the position of the Zn $3d$ states (Table II). The wurtzite and zinc blende band gaps calculated by FEFF are 1.6–1.8 eV, too small in comparison with experiment, but this is consistent with use of the local density approximation to treat electronic correlation and exchange. Surprisingly, despite accurately modeling the modulations in the conduction band and XANES spectroscopy associated with *cubic-hexagonal* polytypism, the experimental trend in band gaps is not reproduced. The position of the Zn $3d$ states is also difficult to calculate accurately, because of the interaction between localized *d*-states and the conduction band.[20] In the present work, and the calculations of Table I, neglect or incomplete treatment of the repulsion term results in the $3d$ states being underbonded.

Although experiment and calculation show that S and Zn *K*-edge absorption spectra cannot be used to distinguish the wurtzite-zinc blende modification [Figs. 2(c) and 2(d)] there are also predicted modulations in the density of unoccupied *p* states (inset to Fig. 3). This is responsible for a small differ-

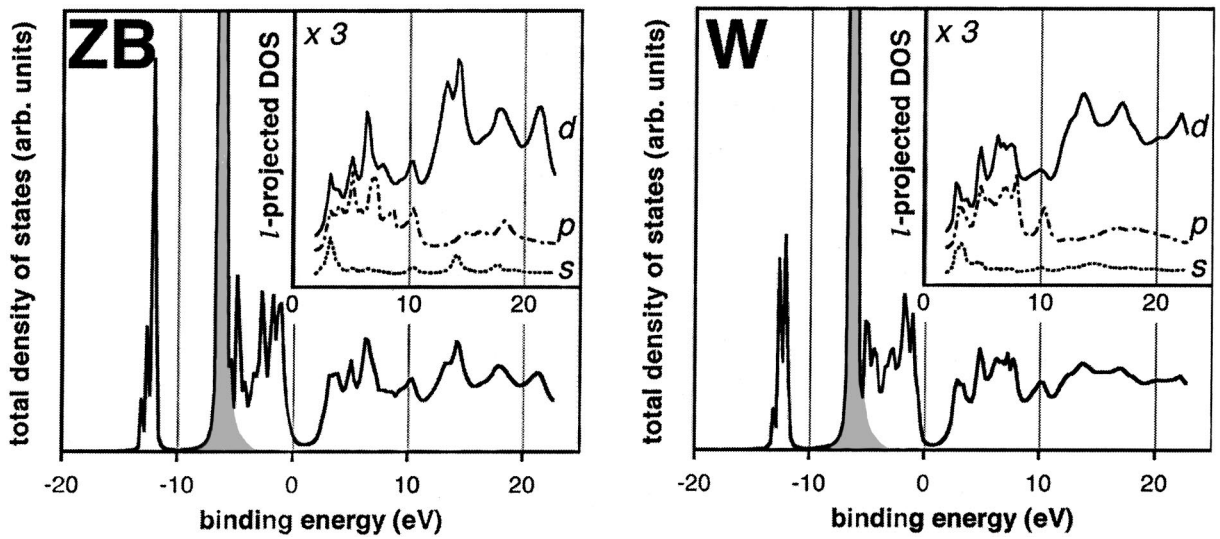

FIG. 3. Electronic density of states (DOS) calculated for zinc blende (ZB) and wurtzite (*W*) polytypes of ZnS. The energy scale is relative to the valence band maximum. Given are the total DOS, and (inset) the *l*-projected unoccupied DOS at the sulfur site, multipled by 3 relative to main graph, and slightly displaced for clarity. The Zn 3*d* bands are shaded. The radii of the clusters used in the calculations are 11.5 Å (ZB, 329 atoms) and 12.27 Å (*W*, 406 atoms).

ence perceptible at the sulfur *K*-edge around 2.482 keV [Fig 2(c)], but such fine-structure shifts are obscured by core hole lifetime broadening at the *K*-edge, discussed below. The removal of core hole broadening by measuring XAS with resonant x-ray emission detection may allow *p* band differences to be resolved.[28]

B. Relevance to x-ray absorption spectroscopy of nanoscale materials

A study of the sensitivity of XAS to polytypism allows a consideration of the volume probed in the x-ray absorption process, relevant for the use of XAS in nanoscale materials. Polytypisms in bulk materials are easily observed, since long-range periodicity allows diffraction approaches, but there exist systems that remain inaccessible to x-ray or electron-diffraction methods, and for which a local (short-range) analysis technique is required. It has been shown that quantum confinement effects may modulate electronic structure at the valence and conduction band edges of semiconducting nanoparticles,[17,29] but there are likely to be additional size-related effects due to crystal structure modification. A small particle size may lead to a change of the most stable crystalline phase,[5] or to distortion.[30] Such ideas have been difficult to test because diffraction patterns from nanoparticles show a substantial broadening as the number of diffracting Bragg planes is dramatically reduced.

X-ray absorption appears naturally suited to the analysis of nanoscale systems, and by combining experiment and calculation we demonstrate that the volume probed by near-edge XAS is on the nanoscale for semiconducting materials. We chose the S $L_{2,3}$ absorption edge, which shows a clear sensitivity for *cubic-hexagonal* polytypism, and is well modeled by calculations. Figure 4 shows the evolution of calculated spectra for increasing cluster size, until convergence and agreement with experiment are reached. It is clear that the absorption lineshape close to the edge is the most sensitive to longer range structure, as expected. Convergence is

TABLE II. Comparison of calculated and experimental band gap E_g and Zn 3*d* binding energies, in eV, relative to the VB maximum. Abbreviations: ZB: zinc blende; *W*: wurtzite; LCGO: linear combination of Gaussian orbitals; LCAO: linear combination of atomic orbitals; OLCAO: orthogonalized linear combination of atomic orbitals; PW: plane-wave pseudopotential method.

Method	Ref., year	E_g		E (Zn3*d*)	
		ZB	W	ZB	*W*
experiment	21, 1977	3.70	3.91	−9.1	-
FEFF	this work	2.16	2.06	−6.19	−6.21
LCGO	22, 1981	2.26	-	−6.4	
LCAO	23, 1985	3.81	3.92	-	-
OLCAO	24, 1993	2.34	-	−6.3	-
PW	25, 1991	1.84	-	−6.40	-
PW	26, 1993	3.55	3.23	−5.8	−5.84

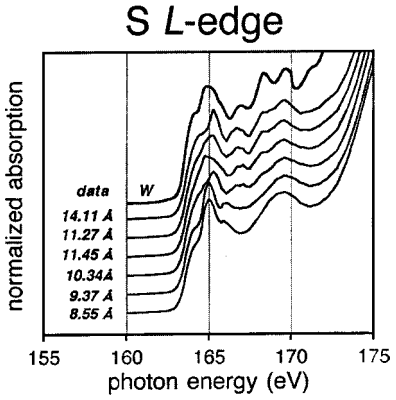

FIG. 4. The effect of cluster size on calculations of x-ray absorption near edge fine structure for *hexagonal* Zn*S*. S $L_{2,3}$ spectra are plotted for successive additional sulfur outer shells. Convergence, and a good agreement with experimental data, are reached at a 14.11-Å radius.

reached at the 14.11-Å radius for wurtzite. This can be taken as an upper limit for this material because, at higher-energy absorption edges, a finite core hole lifetime broadens the fine structure and limits the effective mean free path of the photoelectron. The core hole lifetime and scattering contributions to the total mean free path combine as:[14,31]

$$\lambda_{\mathrm{tot}}=\frac{1}{\frac{1}{\lambda(E)}+\frac{m\Gamma_h}{\hbar k}},$$

where $\hbar^2k^2=2mE$ gives the energy above the mean interstitial potential and $\lambda(E)$ is given by the imaginary part of the exchange potential. Clearly, for S *L*-edge absorption the core hole lifetime width $\Gamma_h\approx 0$ eV. By contrast, at the Zn *K*-edge $\Gamma_h=1.9$ eV,[32] and within 15 eV from threshold, despite large $\lambda(E)$, the resolution is core hole lifetime limited. This behavior is detected in our data, as FEFF convergence at the Zn *K*-edge is obtained for clusters of 9.7 Å. At this calculation size the experimental lineshape is fully reproduced.

V. CONCLUSIONS

By comparing data and calculations we have shown explicitly that x-ray absorption line shapes are linked to the density of unoccupied states, and that these electronic states can be modified by crystal structure changes that do not alter the first shell absorber environment. We summarize the requirements for XANES to be sensitive to crystal polytypism.

(i) That there exists an x-ray absorption edge corresponding to a transition (e.g., *s-p* on *p-d*) for which the final states are modulated by the different symmetries of the polytypes. This is true for *d*-like unoccupied states in ZnS.

(ii) That the mean free path of the photoelectron—including core hole lifetime and extrinsic effects—is sufficient for the photoelectron to probe a volume of the crystal possessing the full site symmetry of the absorber.

This offers a framework to extend these results to other systems, in particular, metallic systems, for which mean free paths are substantially reduced. Given condition (i), there are advantages in acquiring low energy XANES, which give reduced experimental peak broadening and longer photoelectron mean free paths.

ACKNOWLEDGMENTS

This work was based upon research conducted mainly at the Synchrotron Radiation Center, University of Wisconsin-Madison, which is supported by the NSF under Award No. DMR-0084402. Work at the Advanced Photon Source is supported by the U.S. Department of Energy, Office of Science, Office of Basic Energy Sciences under Contract No. W-31-109-ENG-38. We thank SRC staff, especially Mark Bissen. Helpful discussions with John Rehr and Glenn Waychunas are acknowledged. We thank Mumit Khan for large cluster FEFF implementation and Michael Finnegan for assistance with the XRD.

*Present address: Department of Earth and Planetary Sciences, University of California-Berkeley, 455 McCone Hall, California 94720. Email address: bgilbert@eps.berkeley.edu

[1] G. E. Engel and R. J. Needs, J. Phys.: Condens. Matter **2**, 367 (1990).
[2] K. Kim, W. R. L. Lambrecht, and B. Segall, Phys. Rev. B **53**, 16 310 (1996).
[3] J. F. Suyver, S. F. Wuister, J. J. Kelly, and A. Meijerink, Nanoletters **1**, 429 (2001).
[4] M. Labrenz, G. K. Druschel, T. Thomsen-Ebert, B. Gilbert, S. A. Welch, K. M. Kemner, G. A. Logan, R. E. Summons, G. De Stasio, P. L. Bond, B. Lai, S. D. Kelly, and J. F. Banfield, Science **290**, 1744 (2000).
[5] S. B. Qadri, E. F. Skelton, A. D. Dinsmore, J. Z. Hu, W. J. Kim, C. Nelson, and B. R. Ratna, J. Appl. Phys. **89**, 115 (2001).
[6] D. Li, G. M. Bancroft, M. Kasrai, M. E. Fleet, X. H. Feng, K. H. Tan, and B. X. Yang, J. Phys. Chem. Solids **55**, 535 (1994).
[7] D. Li, G. M. Bancroft, M. Kasrai, M. E. Fleet, X. Feng, and K. Tan, Can. Mineral. **33**, 949 (1995).
[8] R. A. D. Pattrick, J. F. W. Mosselmans, and J. M. Charnock, Eur. J. Mineral. **10**, 23 (1998).
[9] K. Lawniczak-Jablonska, R. J. Iwanowski, Z. Golaki, A. Traverse, S. Pizzini, A. Fontaine, I. Winter, and J. Hormes, Phys. Rev. B **53**, 1119 (1996).
[10] Ph. Sainctavit, J. Petiau, M. Benfatto, and C. R. Natoli, Physica B **158**, 3470 (1989).
[11] J. L. Birman, Phys. Rev. **115**, 1493 (1959).
[12] A. L. Ankudinov, B. Ravel, J. J. Rehr, and S. D. Conradson, Phys. Rev. B **58**, 7565 (1998).
[13] B. Ravel, J. Synchrotron Radiat. **8**, 314 (2001).
[14] J. J. Rehr and R. C. Albers, Rev. Mod. Phys. **72**, 621 (2000).
[15] J. Rockenburger, L. Troger, A. Kornowskki, T. vossmeyer, A. Euchmuller, J. Feldhaus, and H. Weller, J. Phys. Chem. B **101**, 2691 (1997).
[16] F. J. Himpsel, U. O. Karlsson, A. B. McLean, L. J. Terminello, F. M. F. de Groot, M. Abate, J. C. Fuggle, J. A. Yarmoff, B. T. Thole, and G. A. Sawatzky, Phys. Rev. B **43**, 6899 (1991).
[17] J. Luning, J. Rockenberger, S. Eisebitt, J.-E. Rubensson, A. Karl,

A. Kornowski, H. Weller, and W. Eberhard, Solid State Commun. **112**, 5 (1999).
[18] L. Ley, R. A. Pollak, F. R. McFeely, S. P. Kowalczyk, and D. A. Shirley, Phys. Rev. B **9**, 600 (1974).
[19] L. Zhou, T. A. Callcott, J. J. Jia, D. L. Ederer, and R. Perera, Phys. Rev. B **55**, 5051 (1997).
[20] S.-H. Wei and A. Zunger, Phys. Rev. B **37**, 8958 (1988).
[21] *Electronic Structure of Solids: Photoemission Spectra and Related Data*, edited by T. C. Chiang, K. H. Frank, H. J. Freund, A. Goldmann, F. J. Himpsel, U. Karlsson, R. C. Leckey, W. D. Schnieder, and E.-E. Koch, Landolt-Börnstein, New Series, Group III, Vol. 23, Pt. A (Springer-Verlag, Berlin, 1994).
[22] C. S. Wang and B. M. Klein, Phys. Rev. B **24**, 3393 (1981).
[23] M.-Z. Huang and W. Y. Ching, Phys. Chem. Solids **46**, 977 (1985).
[24] M.-Z. Huang and W. Y. Ching, Phys. Rev. B **47**, 9449 (1993).
[25] J. L. Martins, N. Troullier, and S.-H. Wei, Phys. Rev. B **43**, 2213 (1991).
[26] P. Schroer, P. Kruger, and J. Pollmann, Phys. Rev. B **47**, 6971 (1993).
[27] *Physics and Chemistry of II–VI Compounds*, edited by M. Aven and J. S. Prener (North-Holland, Amsterdam, 1967).
[28] K. Hamalainen, D. P. Siddons, J. P. Hastings, and L. E. Berman, Phys. Rev. Lett. **67**, 2850 (1991).
[29] A. P. Alivisatos, Science **271**, 933 (1996).
[30] K. S. Hamad, R. Roth, J. Rockenberger, T. van Buuren, and A. P. Alivisatos, Phys. Rev. Lett. **83**, 3474 (1999).
[31] D. G. Stearns, Philos. Mag. B **49**, 541 (1984).
[32] Keski-Rahkonen and M. O. Krause, At. Data Nucl Data Tables, **14**, 139 (1974).